APPLICATION OF SA AND VFSA GLOBAL OPTIMIZATION ALGORITHMS FOR SEARCH OF THE 2-D CRS STACKING PARAMETERS

G. Garabito, J. C. Cruz, and P. Hubral

email: *german@ufpa.br*

keywords: *Stacking, CRS parameters, coherency, Optimization*

ABSTRACT

The Common Reflection Surface Stack (CRS) method simulates zero-offset (ZO) sections by means of summing the amplitudes of seismic events in the multicoverage data by using a stacking surface. For 2-D media, this stacking surface depends on three kinematics attributes of two hypothetical waves at the point of emergency of the normal incidence central ray, namely, the emergency angle of the normal ray, the radius of curvature of the Normal Incidence Point Wave and the radius of curvature of the Normal Wave. The optimization problem in the CRS method consists in determining, from the multicoverage seismic data, the three CRS parameters associated to each sample point of ZO section to be simulated. The simultaneous determination of these parameters can be made by means of multidimensional global search process (or global optimization), using as objective function some coherence criterion. In this work we present the results of the application of two global optimization algorithms to search the CRS parameters, e.g. the Simulated Annealing and Very Fast Simulated Annealing. Unlike the old strategies that search for the CRS parameters using three or more steps, in this work the search strategy has only one step, i.e. the three CRS parameters are obtained simultaneously.

INTRODUCTION

Through the seismic stacking methods it can be obtained images of the geological structures in the subsurface, by simulation of ZO section from multicoverage seismic data. The Common Midpoint (CMP) stack is the method commonly used in the oil exploration to simulate ZO seismic sections.
The CRS stacking method (Müller (1998); Jäger et al. (2001); Mann (2001); Garabito et al. (2001a),b) was presented as a more robust alternative to simulate ZO sections. Like the CMP stack, the CRS method does not dependent on a macro-velocity model and provides higher quality images in heterogeneous media.

The CRS stacking method consists of summing the amplitudes of the multicoverage seismic data along the stacking surface. This surface is defined by a hyperbolic paraxial traveltime approximation, that depends on three parameters: the emergence angle of the normal (central) ray (with respect to the normal to the measurement surface), β_0, and the wavefront curvatures of two hypothetical waves, the so-called Normal-Incidence-Point (NIP) wave ($K_{NIP} = 1/R_{NIP}$) and Normal (N) wave ($K_N = 1/R_N$), as defined by Hubral (1983).

The fundamental problem of the 2-D CRS stacking method consists in determining three CRS parameters from multicoverage seismic data. The parameter triplet is associated to each sample of the ZO section in time domain. The determination of these parameters (β_0, K_{NIP}, K_N) from pre-stack data can be accomplished by using optimization processes where the objective function is a coherence measure (Semblance). Garabito et al. (2001a,b) determined these CRS parameters by applying a combination of global and local optimization processes in three-steps (3S), by using the Simulated Annealing algorithm

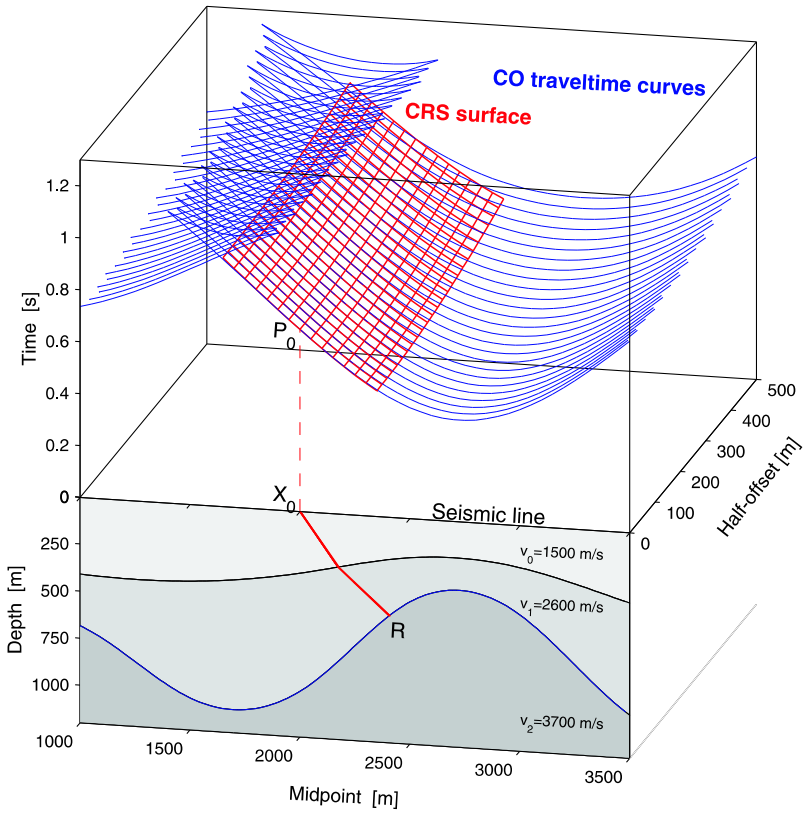

Figure 1: Top: CRS stack traveltime surface for point P_0 in the ZO plane. The blue lines are the modeled Common-Offset traveltimes for the second reflector. Bottom: Model with two homogeneous layers above a half-space separated by a curved interface.

(Corana et al., 1987) for the global search and Quasi-Newton algorithm (Gill et al., 1981) for the local search.

In this work the CRS parameters (β_0, K_{NIP}, K_N) are searched-for by using an one-step (1S) optimization procedure, by which these are determined simultaneously. In order to evaluate the computational performance of the 1S-CRS stack we compare the results of the SA and VFSA optimization algorithms, when applied to the Marmousi data set. We also compare the application of 1S-CRS stack to the Marmousi data, by using the SA algorithm, with respect to the 3S-CRS stack strategy.

THEORETICAL ASPECTS

CRS stack

The CRS stacking surface is represented by a hyperbolic paraxial traveltime approximation given by (**?**)Tygel:97)

$$t^2(x_m, h) = \left(t_0 + \frac{2\sin\beta_0}{v_0}\,(x_m - x_0)^2\right)^2 + \frac{2\,t_0\cos^2\beta_0}{v_0}\left((x_m - x_0)^2 K_N + h^2 K_{NIP}\right). \qquad (1)$$

In equation 1, t_0 is the two-way traveltime of the normal ray and v_0 is the near-surface velocity associated with the normal ray. $x_m = (x_S + x_G)/2$ and $h = (x_G - x_S)/2$ are the midpoint and half-offset coordinates between the source and receiver, respectively. x_S and x_G are the horizontal coordinates of the source and receiver pair (S, G), respectively. K_N and K_{NIP} are the hypothetical wavefront curvatures, and β_0 is the emergence angle of the normal (central) ray (1).

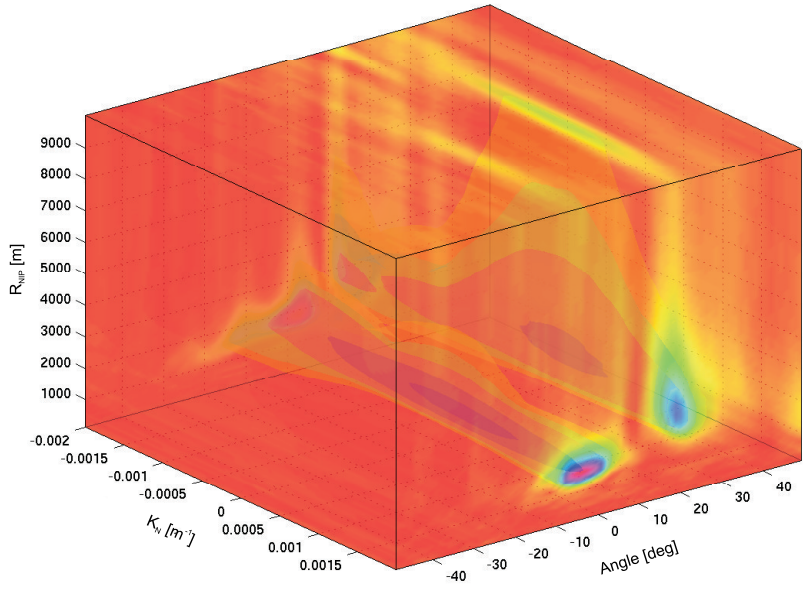

Figure 2: Cube of coherence values obtained with equation 1 for the point of the ZO section of the Marmousi data that corresponds to a conflicting dip situation. The minimum value of coherence is located in $\beta_0 = -3.03^0$, $R_{NIP} = 16245m$ and $K_N = 0.00054545m^{-1}$.

Figure 1 shows the CRS stacking surface (red line) associated to a sampling point P_0 corresponding to a central ray that emerges in X_0. This surface is defined by equation (1), where the parameters (β_0, K_{NIP}, K_N) associated to the central ray were obtained by forward modeling. In this Figure, the lines blue represent the primary reflection traveltimes associated to the second reflector for different offsets between sources and receivers. Stacking seismic events in every CRS surface and putting the result in the ZO sampling point, we obtain the ZO section simulated by the CRS method. In practice, these parameters (β_0, K_{NIP}, K_N) are determined from seismic data by using optimization methods.

Global optimization of the CRS parameters

The main problem to implement the CRS method consists of determining from multicoverage seismic data, the three parameters (β_0, K_{NIP}, K_N) associated to each sampling point of the ZO section to be simulated. The simultaneous determination of these parameters can be accomplished through optimization processes using as objective function some criterion of coherence of the seismic data. In this work we use the Semblance function (Neidell and Taner, 1971) which is normalized output-to-input energy ratio, is given by

$$S = \frac{1}{M} \frac{\sum_t \left(\sum_{i=1}^{M} f_{i,t(i)} \right)^2}{\sum_t \sum_{i=1}^{M} f_{i,t(i)}^2}, \tag{2}$$

where $f_{i,t(i)}$ is the amplitude value on the ith trace at two-way traveltime $t(i)$. Here, M is the number of traces in the CMP gather. Semblance is a coherence measure normalized with values between 0 and 1.

Figure 2 shows the semblance function used in the optimization processes by the CRS method. In this Figure, we observe a 3-D graphic with coherence values for the parameters $(\beta_0, R_{NIP} = 1/K_{NIP}, K_N)$ symmetrically distributed along the interval, $-0.002m^{-1} \leq K_N \leq 0.002m^{-1}$. Therefore, the coherence volume for these intervals is defined as the search-space to optimize the CRS parameters.

The coherence cube of Figure 2 corresponds to the sampling point $P_0(t_0 = 1.27s, x_0 = 7375m)$ of the

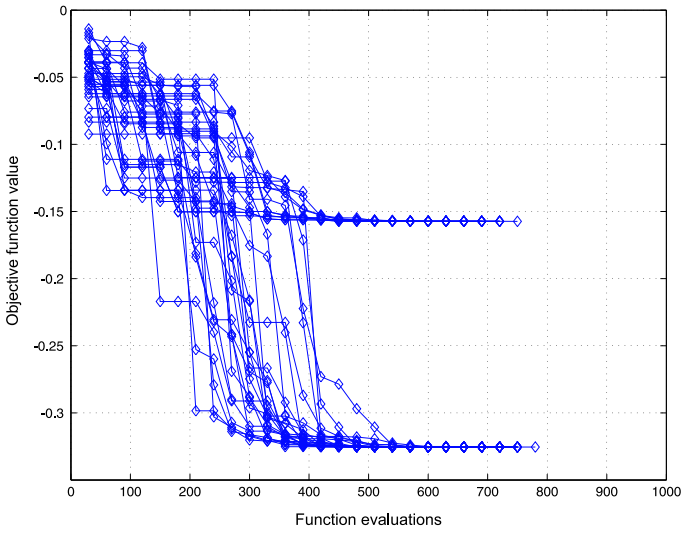

Figure 3: Performance of SA algorithm in minimizing the CRS objective function for three-parameters.

ZO section of the Marmousi dataset that corresponds to a situation with intersection of seismic events with different angles, so-called conflicting dip situation. The global minimum or smaller value of coherence is located in $\beta_0 = -3.03^0$, $R_{NIP} = 1624.5m$ and $K_N = 0.00054545m^{-1}$. These parameter triplet defines the CRS stacking surface that best fit the seismic events of the multicoverage seismic data and correspondents to one of the events with conflicting dip of the ZO section.

NUMERICAL RESULTS

For the optimization tests of the CRS parameters were used the Marmousi synthetic dataset (Bourgeois et al., 1991).

The obtained results represent several tests accomplished with each one of the studied optimization algorithms. The horizontal axis represents the number of evaluations and the vertical axis is the value of the objective function (negative Semblance). These results show the evolution of the algorithms until the global minimum.

Simulated Annealing (SA) algorithm

In the SA method (Corana et al., 1987), the minimization process begins with an initial value of temperature $T = T_0$ and, in general, a vector of initial parameters ($\mathbf{p} = \mathbf{p}_0$) randomly generated. Then, given an initial point $\mathbf{p}$ and the respective value of the objective function $\mathbf{f}(\mathbf{p})$, the generation of a test point is accomplished through the application of a disturbance in each element of $\mathbf{p}$. If the value of $\mathbf{f}(\mathbf{p}^{'})$ is smaller than $\mathbf{f}(\mathbf{p})$, then the point $\mathbf{p}$ is substituted for $\mathbf{p}'$ and the algorithm has a descending displacement. When the value $\mathbf{f}(\mathbf{p}^{'})$ of the test point has a value similar or larger than $\mathbf{f}(\mathbf{p})$, a criterion of probability decides if these test point is accepted or not. If it be accepted, then $\mathbf{p}$ and $\mathbf{f}(\mathbf{p})$ are substituted for $\mathbf{p}'$ and $\mathbf{f}(\mathbf{p}^{'})$, respectively, and the algorithm has an ascending displacement.

In this algorithm we used an initial temperature of $T_0 = 0.1$, with a decline factor $r_T = 0.85$ and value of tolerance of the error $\epsilon = 0.001$.

Figure 3 displays the performance of the SA algorithm to search the parameters (β_0, K_{NIP}, K_N).

Very Fast Simulated Annealing (VFSA) algorithm

This algorithm follows the same search procedure of the SA algorithm. The VFSA algorithm was proposed by Ingber (1989) introducing modifications to the pattern algorithm also known as Boltzamann Annealing

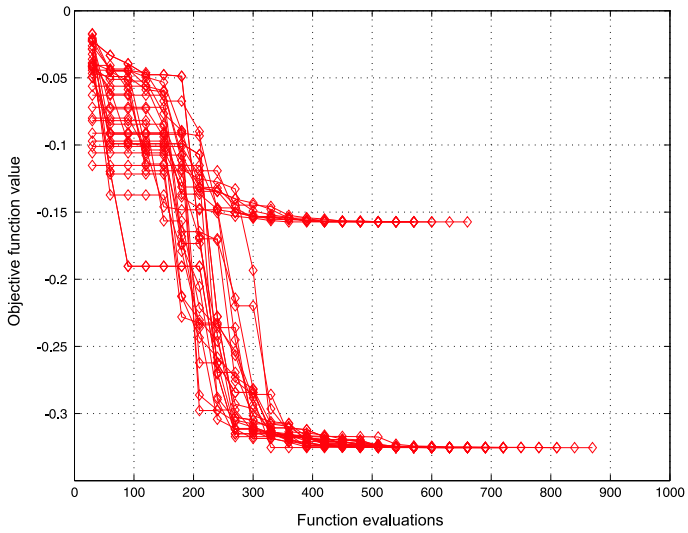

Figure 4: Performance of VFSA algorithm in minimizing the CRS objective function for three-parameters.

(BA) algorithm, with the objective of improving the performance. These modifications refer to the form of disturbance of the parameters and the sequence of cooling of the temperature.

With this algorithm we use $T_0 = 1,5$, $k = 30$ and $c_i = 0.25$ for the three-dimensional search. Figure 4 illustrates the performance of VFSA algorithm.

DISCUSSION OF THE RESULTS

Analyzing the results above, we can observe that the VFSA algorithm is more efficient to find the minimum value of the objective function for the three parameters, with an average of 350 evaluations of the function. However, due to the fast decreasing of the temperature this algorithm can be restricted to the local minimum and in other cases gets to leave the local minimum after a certain number of iterations. This implicates that VFSA algorithm does not have great effectiveness in determining the global minimum, but it can reach the global minimum with a great number of tests. The SA algorithm has a slower decreasing of temperature than VFSA algorithm, and it has an average of 450 evaluations of the objective function to find the global minimum. Like the VSFA, the SA algorithm also keep restricted to the local minimum in several tests, reducing effectiveness in estimating the global minimum. But, we can observe that the SA algorithm is more robust than VFSA because it has a larger number of success in finding the global minimum.

CRS stack

We present simulated ZO sections windows from Marmousi dataset by using an one-step CRS stack, Figures 5 and 6, with the SA and VFSA, respectively. In general, these results show that SA algorithm is more robust, because it converges more efficiently for the global minimum, and provide a better definition of the seismic events in respect to the result obtained by the VFSA optimization algorithm. For some estimates of CRS parameters the VFSA does not reach the global minimum, even for seismic events with high coherence.

Figures 7 and 8 display a comparison between the one-step with SA and three-steps CRS strategies, applied to the Marmousi dataset. We observe that the result of the one-step show a better resolution with much better continuity of reflector horizons.

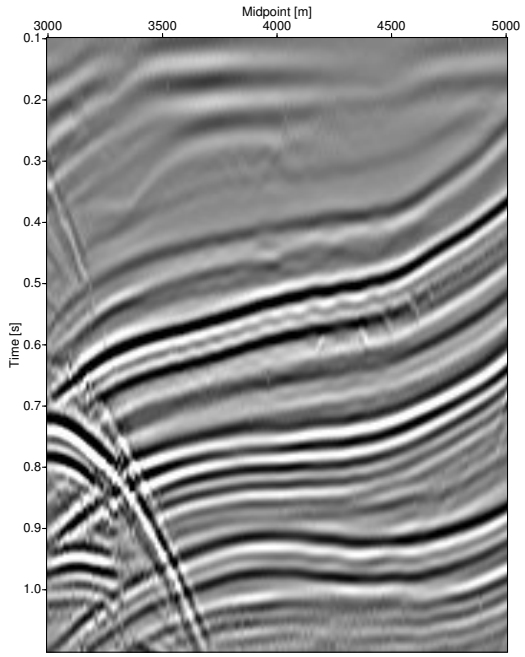

Figure 5: Closeup of simulated ZO section from Marmousi dataset obtained by using 1S-CRS stack with the SA algorithm.

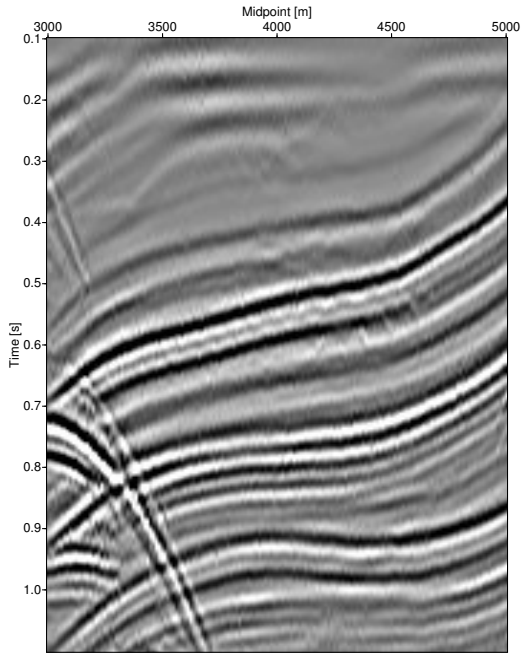

Figure 6: Closeup of simulated ZO section from Marmousi dataset obtained by using 1S-CRS stack with the VFSA algorithm.

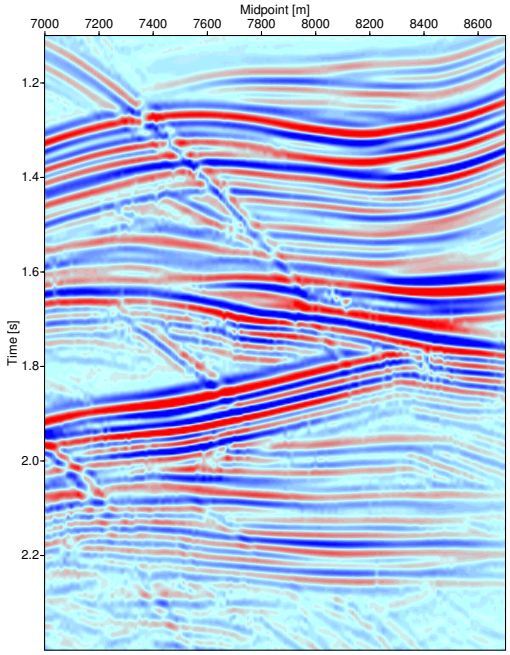

Figure 7: Closeup of simulated ZO section from Marmousi dataset obtained by using 1S-CRS stack with SA algorithm.

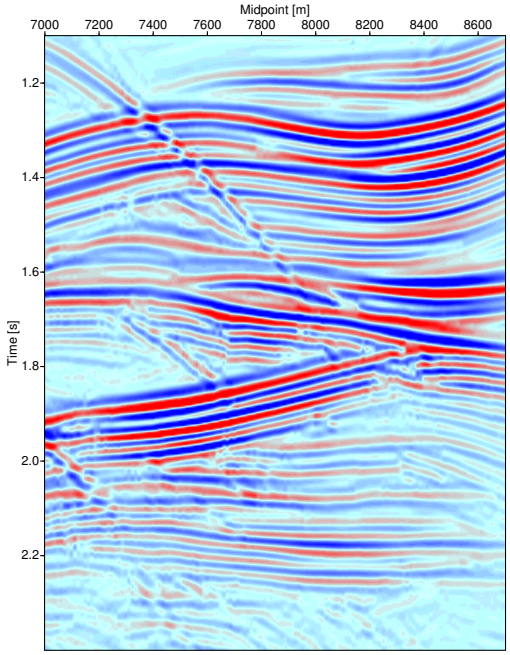

Figure 8: Closeup of simulated ZO section from Marmousi dataset obtained by using 3S-CRS stack with SA and quasi-Newton algorithms.

CONCLUSIONS

The performance test of the optimization algorithm VFSA and SA show that both keep restricted to the local minimum in several tests. But for a large number of tests both converges to global minimum. The VFSA is more effective than SA algorithm, because it reaches the global minimum for a small number of objective function evaluation. By comparison of simulated ZO sections we observe that SA algorithm is more robust, because it provides a better definition of the seismic events in respect to the result obtained by the VFSA optimization algorithm. We observe that the result of the one-step CRS stack show a better resolution with much better continuity of reflector horizons, in comparison with the results of the three-steps CRS stack strategy.

ACKNOWLEDGMENTS

The authors thank the support received during the accomplishment of this work, of the following institutions: CAPES, CNPq and UFPA.

REFERENCES

Bourgeois, A., Bouget, M., Lailly, P., Poulet, M., Ricarte, P., and Versteeg, R. (1991). Marmousi, model and data. *In: 52nd. EAEG meeting, Proceedings of the Workshop on Practical Aspects of Seismic Data Inversion, Copenhagen*, page 56.

Corana, A., Marchesi, M., Martini, C., and Ridela, S. (1987). Minimizing multimodal functions of continuous variables with "simulated annealing" algorithm. *ACM Transactions on Mathematical Sofware*, 13(3):262–280.

Garabito, G., Cruz, J. C. R., Hubral, P., and Costa, J. (2001a). Common reflection surface stack by global optimization. *71st Annual Internat. Mtg., Soc. Expl. Geophys. Expanded Abstracts*.

Garabito, G., Cruz, J. C. R., Hubral, P., and Costa, J. (2001b). Empilhamento de superfície de reflexão comum com mergulhos conflitantes. *7th International Congress of the Brazilian Geophysical Society*.

Gill, P. E., Murray, W., and Wright, M. H. (1981). Practical optimization. *Academic Press, London and NY.*

Hubral, P. (1983). Computing true amplitude reflections in a laterally inhomogeneous earth. *Geophysics*, 48:1051–1062.

Ingber, L. (1989). Very fast simulated re-annealing. *Math1. Comput. Modelling*, 12(9):967–973.

Jäger, R., Mann, J., Höcht, G., and Hubral, P. (2001). Common reflection surface stack: Image and attributes. *Geophysics*, pages 97–109.

Mann, J. (2001). Common-reflection-surface stack and conflicting dips. *71th Annual Internat. Mtg. Soc. Expl. Geophys. Extended Abstracs.*, 13(3):262–280.

Müller, T. (1998). Common reflection surface stack versus nmo/stack and nmo/dmo/stack. *60th Mtg. Eur.Assoc. Expl. Gophys., Extended Abstracts.*

Neidell, N. and Taner, M. (1971). Semblance and other coherency measures for multichannel data. *Geophysics*, 36:482–497.